

pubs.acs.org/IECR Article

Process Designs for Separating R-410A, R-404A, and R-407C Using Extractive Distillation and Ionic Liquid Entrainers

Ethan A. Finberg and Mark B. Shiflett*



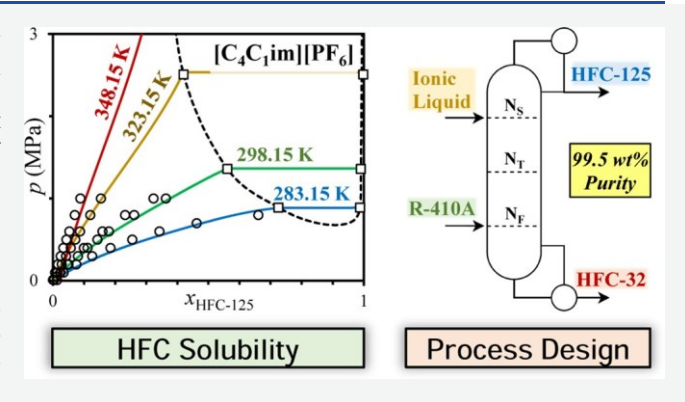
ACCESS |

Metrics & More

Article Recommendations

Supporting Information

ABSTRACT: Hydrofluorocarbon refrigerants are being phased out over the next two decades due to their high global warming potential. To separate and recycle refrigerants that form azeotropic mixtures, current distillation methods are inadequate and a new technology is required. Extractive distillation using an ionic liquid as the entrainer offers a solution. Vapor liquid equilibria data refrigerants difluoromethane (HFC-32), chlorodifluoromethane pentafluoroethane (HCFC-22), (HFC-125), 1,1,1-trifluoroethane (HFC-143a), and 1,1,1,2tetrafluoroethane (HFC-134a) in ionic liquids 1-ethyl-3- $\label{eq:methylimidazolium} methylimidazolium \ bis(trifluoromethylsulfonyl)- \ imide \\ ([C_2C_1im][Tf_2N]) \ and \ 1-butyl-3-methylimidazolium \ hexa$ fluorophosphate ([C₄C₁im][PF₆]) were fit with the Peng-



Robinson equation of state to simulate the separation of four

azeotropic refrigerant mixtures (R-404A, R-407C, R-410A, and R-410A + HCFC-22) and to develop rate-based and equilibrium models in ASPEN Plus. Process flow diagrams were developed and optimized based on a set of physical and chemical constraints. The goal was to optimize the parameters to achieve refrigerant grade (>99.5)

1. INTRODUCTION

Hydrofluorocarbons (HFCs) have been used as refrigerants globally since the 1990s and replaced chlorofluorocarbons hydrochlorofluorocarbons (HCFCs), which were linked to the depletion of the Earth's ozone layer. Even though HFCs have zero ozone depletion potential, some HFCs have a high global warming potential (GWP) ranging from 1000 to 5000^{1} on a 100-year basis where CO_2 = 1.0. The European Fluorinated Greenhouse Gas (EU F-Gas) Regulations,2 the Kigali Amendment to the Montreal Protocol,^{3,4} and most recently in 2020, the American Innovation and Manufacturing (AIM) Act,⁵ all plan to reduce climate change by significantly reducing the production and use of HFCs over the next two decades. The refrigerant industry is currently transitioning to the next-generation refrigerants, hydrofluoroolefins (HFOs), and HFO/HFC refrigerant blends, to replace HFCs in many applications.⁶ This will require the recycling and repurposing of HFC mixtures; however, many are azeotropic or near azeotropic (i.e., R-404A, 7 R-407C, 8 and 8 $R-410A^{9,10}$), making the separation difficult or impossible using current distillation methods. HFCs such as HFC-32 with a lower GWP = 677 can be used in new refrigerant mixtures such as R-454 composed of HFO-1234yf (2,3,3,3-tetrafluoropropene) and HFC-32 fluoromethane). Higher GWP HFCs such as HFC-125 (GWP

 $\stackrel{\cdot}{=}$ 3170) and HFC-143a (GWP = 4800) can be potentially

utilized as new feedstocks for fluorinated polymers. Project EARTH (Environmentally Applied Research

Toward Hydro-

fluorocarbons) is a multi-university effort involving the University of Kansas, the University of Notre Dame, Texas A&M University, and Rutgers University funded by the National Science Foundation (NSF), which aims to develop environmentally responsible materials and technology to separate azeotropic HFC mixtures and recycle the pure component refrigerants.

Extractive distillation¹¹ is the most widely used technology for the separation of homogeneous azeotropic mixtures or solvents with similar boiling points.¹² Extractive distillation separations include organic/water, olefin/paraffin (alkene/alkane), aliphatic/aromatic hydrocarbons, and aromatic/ aromatic hydrocarbons.¹³ Extractive

distillation uses an additional solvent, an entrainer, to alter the liquid phase properties and modify the volatility of each component, resulting in a more efficient separation. The entrainer absorbs one of the components to carry the solute to the bottom of the column while the other component is distilled out the top of the column. The entrainer and the absorbed component are

Received: July 19, 2021 Revised: September 20, 2021 Accepted: October 13, 2021



© XXXX American Chemical Society

Α

https://doi.org/10.1021/acs.iecr.1c02891 Ind. Eng. Chem. Res. XXXX, XXX, XXX–XXX fed into another unit operation, usually a flash column or second stripping column, to purify the solute and recover the entrainer. Entrainers are typically high boiling solvents that make recovery and recycling simple and efficient. Extractive distillation columns contain either sieve trays or structured packing.

The defining characteristics for an entrainer are miscibility

with the feed, absorption selectivity between the components, and low volatility. Experimentally, these can be measured using gravimetric and volumetric techniques, chromatography, and ebulliometry. The entrainer should not form any azeotropes with the feed components. In most cases, the solvent is much less volatile than the feed components to ensure an easy solvent recovery and a large difference in component concentrations. A low miscibility between the entrainer and components can lead to two-liquid phases and should be avoided. There are five types of entrainers used in extractive distillation: liquid solvents, solid salts (or dissolved salts), a mixture of liquid solvents and solid salts, hyperbranched polymers, and ionic liquids (ILs).¹⁴ Organic liquid solvents have been the primary choice for entrainers, but ILs have shown higher selectivity for many processes. 15,16

ILs are typically composed of a large organic cation and an inorganic anion with a melting point defined to be below 100

 $^{\circ}\text{C.}^{17}$ Room temperature ILs are liquids at room temperature.

Many ILs have high thermal and chemical stability with a wide liquid range and negligible vapor pressure that makes them ideal as entrainers for extractive distillation. One trade-off of using extractive distillation is the risk of the entrainer contaminating the distillate product. ILs, unlike other organic solvents, have extremely low vapor pressure (e.g., $<1 \times 10^{-5}$ Pa) that significantly reduces the amount of IL in the distillate. In addition, ILs can be efficiently recycled due to the low volatility. Another interesting feature of ILs is the ability to tune properties, such as density, viscosity, and gas solubility for different components, to maximize separation efficiency by selecting the appropriate cation and anion. Experimental equilibrium data [e.g., activity coefficients at infinite dilution, vapor-liquid equilibrium (VLE), and liquid-liquid equili- brium (LLE) of binary and ternary systems] are available in the Dortmund Data Bank and ILThermo NIST Database. 18 Extensive studies and reviews on gas solubility in ILs¹⁹⁻²¹ have been published, but only a few works describe the separation of azeotropic mixtures using ILs as entrainers for extractive distillation.²² ILs were first introduced as entrainers in 2001 by the BASF Chemical Company and patented in 2004 by Arlt et al. 23,24 To the best of our knowledge, BASF 25 and Eindhoven University of Technology²⁶ are the only two institutions that have published experimental results for extractive distillation using ILs.

Process designs for extractive distillation with IL entrainers

have been investigated for several systems, mostly for aliphatic/aromatic hydrocarbon separation. Navarro et al. have proposed a total of five process designs for the separation of benzene/cyclohexane,²⁷ benzene/methylcycloalkanes,²⁸ cyclohexane/cyclohexene,²⁹ toluene/*n*-heptane,³⁰ and the dear- omatization of pyrolysis gasoline.³¹ Other authors have also modeled benzene/cyclohexane³² and the aromatic-aliphatic separation from naphtha.³³ Designs for dehydration from systems such as ethanol,³⁴⁻³⁹

tetrahydrofuran,³⁷ *tert*-butyl alcohol,⁴⁰ acetonitrile,⁴¹ and *iso*-propanol^{42,43} have also been investigated with extractive distillation using ILs. Other proposed processes include the use of ILs to separate

acetone/methanol,42 cyclopentane/neohexene.44 *n*-heptane/ methylcyclohexane, 45 and ethyl acetate/ethanol.46 However, only three proposed designs have been published for the separation of low boiling components with an IL entrainer [e.g., dioxide/ethane,47 dioxide,48 tetrafluoroethylene/carbon (HFC-32)/pentafluoroethane difluoromethane (HFC-125)].⁴⁹ Recently, Asensio-Delgado et al. published a summary of all references involving provided process designs for refrigerants.⁵⁰ the solubility of fluorinated carbons in ILs, and separating

This study analyzes the separation of low boiling components in binary mixture R-410A and ternary mixtures: R-404A, R-407C, and R-410A mixed with 10 wt % chlorodifluoromethane (HCFC-22). R-410A was the replace- ment for HCFC-22 in residential air-conditioning systems, and recyclers find that these two refrigerants often get mixed together. The compositions for R-404A, R-407C, and R-410A are shown in Table 1 and consist of the components:

Table 1. R-404A, R-407C, and R-410A Components and Composition

component	R-404A (wt %)	R-407C (wt %)	R-410A (wt %)
HFC-32		23	50
HFC-125	44	25	50
HFC-134a	4	52	
HFC-143a	52		

difluoromethane (HFC-32), pentafluoroethane (HFC-125), 1,1,1,2-tetrafluoroethane (HFC-134a), and 1,1,1-trifluoro- ethane (HFC-143a). Each refrigerant mixture also contains at least one

binary azeotrope (e.g., R-404A has binary azeotrope HFC-125 + HFC-143a and R-407C and R-410A have binary azeotrope HFC-32 + HFC-125).^{51,52} In addition, other azeotropes exist such as HFC-32 + HFC-143a, and for the mixture of R-410A with HCFC-22, an azeotrope exists between HFC-125 + HCFC-22. No ternary azeotropes exist with R-404A, R-407C, or R-410A mixed with HCFC-22. ILs can be used to separate HFCs,^{53,54} and extractive distillation will be required to break the binary azeotropes in these refrigerant mixtures.⁵⁵

ILs have high solubility for certain HFCs and HCFCs and are excellent candidates as entrainers. 56,57 In this work, the ILs, 1-ethyl-3-methylimidazolium bis(trifluoromethylsulfonyl)- imide ([C_2C_1 im][T_2 N]) and 1-butyl-3-methylimidazolium hexafluorophosphate ([C_4C_1 im][P_6]) were selected as entrainers because vapor-liquid equilibria data were available for these ILs and the refrigerants of interest in this study. In addition, the ILs also have a fairly low viscosity (e.g., [C_2C_1 im][T_2 N] = 33.4 mPa's at 25 ° C_3 8 and [C_4C_1 im][P_6]

= 217.7 mPa's at 25 °C⁵⁹) and good thermal stability (e.g., [C₂C₁im][Tf₂N] decomposition onset at 222 °C in air and [C₄C₁im][PF₆] decomposition onset at 248 °C in

air).⁶⁰ In this work, reboiler temperatures were maintained below 135

°C, which is a conservative temperature limit considering the onset of decomposition temperatures for both $ILs.^{61,62}$ The $[C_2C_1im][Tf_2N]$ is considered the preferred entrainer since it has the lowest viscosity, the highest thermal stability, and is the most stable in the presence of water at elevated temperatures.⁶³ The other ionic liquid $[C_4C_1im][PF_6]$ is also stable at operating temperatures described in this work and in some cases demonstrates a higher selectivity for HFC-32 from ethane-based refrigerants such as HFC-125 and HFC-143a.

Common lubricants used in air conditioning and refriger- ation systems, such as polyalkylene glycol, ⁶⁴ pentaerythritol tetranonanoate, ⁶⁵ and polyvinyl ether 68, ⁶⁶ were found to have a high solubility for HFCs and were also considered as alternative entrainers to ILs. However, these lubricants had smaller differences in solubility for the HFCs of interest in this work compared with the ILs. ⁶⁷ In addition, the lubricants have a much higher molecular weight than ILs that leads to a low mass fraction solubility and a higher solvent-to-feed ratio in extractive distillation applications.

The goal of this project was to design process flow diagrams

using Aspen Plus V10 for separation of azeotropic HFC mixtures such as R-404A, R-407C, R-410A, and R-410A with HCFC-22 to obtain a minimum purity of 99.5 wt % for each component. Separation of the ternary mixtures consisted of a multistep distillation process involving conventional distillation to remove a relatively high boiling component in the ternary mixture, extractive distillation to isolate a binary mixture of azeotropic refrigerants, and a flash vessel for IL recycle. Simulations were conducted using both equilibrium and rate- based models. The ionic liquid $[C_2C_1im][Tf_2N]$ was tested first and if the desired purity for each component could not be achieved then $[C_4C_1im][PF_6]$ was also evaluated.

2. THERMODYNAMIC MODEL

The Peng–Robinson equation of state (PR-EoS), 68,69 shown in eq 1, was used to define the equilibrium of the system by fitting experimental data for HFC-32, HCFC-22, HFC-125, HFC-134a, and HFC-143a in [C₄C₁im][PF₆] and [C₂C₁im]- [Tf₂N].

$$P = \frac{RT}{V - b} - \frac{a}{V(V + b) + (V - b)}$$
(1)

The PR-EoS parameters, a and b, are a function of the pure component critical properties and Boston-Mathias mixing parameters k_{ij} and l_{ij} , shown in eqs 2 and 3.

$$k = k^{(1)} + k^{(2)}T + \frac{-ij}{}$$

$$i^{j} \quad i^{j} \quad i^{j} \quad T$$

$$l_{ij} = l^{(1)} + l^{(2)}T + \frac{-ij}{}$$

$$i^{j} \quad i^{j} \quad T$$
(2)

The IL physical properties (T_b and MW), critical properties (T_c , P_c , V_c , and ideal gas heat capacities, $\Delta C_{P,IG}$, are required in order to regress the VLE data using the PR-EoS in the ASPEN simulation. The boiling point temperature, T_b , and critical properties for the ILs are considered pseudo-properties because ILs decompose before reaching their boiling point or critical point. Valderrama and Robles^{70,71} presented the group contribution method to define critical property values for 50 different ILs, and the estimated values for [C₂C₁im][Tf₂N] and [C₄C₁im][PF₆] are summarized in Table 2. Ge et al.⁷² generated group contribution parameters to predict $\Delta C_{P,IG}$ for ILs as a function of temperature using the Joback method, and $\Delta C_{P,IG}$ regressions as a function of temperature are provided in Figure S1 in the

Table 2. Physical Properties for ILs

nam e	$[C_2C_1im][Tf_2N]$	$[C_4C_1\mathrm{im}][PF_6]$		
formula	$C_8H_{11}N_3F_6S_2O_4$	$C_8H_{15}N_2PF_6$		
MW (g mol ⁻¹)	391.3	284.2		
$T_{\rm b}$ (K)	816.7	554.6		
$T_{\rm c}$ (K)	1249.3	719.4		
$P_{\rm c}$ (MPa)	3.27	1.73		
$V_{\rm c}$ (cm 3 mol $^{-1}$)	875.9	762.5		
$Z_{ m c}$	0.2753	0.2203		
Ω	0.2157	0.7917		

Values for all binary parameters k_{ij} and l_{ij} with $[C_2C_1\text{im}][Tf_2N]$ and $[C_4C_1\text{im}][PF_6]$ are provided in Table S1 in the Supporting Information.

Table S1 in the Supporting Information.
The PTx for HFC-32, HFC-125, and HFC-134a in $[C_2C_1im][Tf_2N]$ are shown in Figure S2,^{56,75,76} and the PTx for HCFC-22 in [C₂C₁im][Tf₂N] and [C₄C₁im][PF₆] are shown in Figure S3⁷⁷ in the Supporting Information. There is no literature data for the solubility of HFC-143a in $[C_2C_1im][Tf_2N]$, so it was assumed to be the same as the solubility of HFC-143a in [C₄C₁im][PF₆]. The solubility of HFC-125 and HFC-143a is similar in ionic liquid [C₄C₁im]- [PF₆]. Also, the solubility of HFC-125 is similar in both ILs $[C_4C_1im][PF_6]$ and $[C_2C_1im][Tf_2N]$; therefore, it is a reasonable assumption that the solubility of HFC-143a will also be similar to the solubility of HFC-125 in $[C_2C_1im]$ - $[Tf_2N]$, particularly at low solubilities, which is the case for both refrigerants. Once the global PTx phase behavior over the entire composition range was calculated and the heat capacities correlated, the equilibrium separation process was simulated.

LLE was observed in the *PTx* phase behavior (see Figure 1) for HFC-125, HFC-134a, and HFC-143a but not with HFC-32.

3. EQUILIBRIUM AND RATE MODELS

3.1. Equilibrium Model. Equilibrium models were based on the MESH (material balances, equilibrium, summation

equations, and heat balances) equations to calculate the flow

rates, compositions, temperatures, and pressures at each stage. The model assumed that each stage was at equilibrium with

equilibrium with the inlet and outlet streams in order to determine the number of theoretical stages, N needed to achieve the

separation. Physical trays are rarely at equilibrium; therefore, Supporting Information.

Experimental PTx data collected for HFC solubility with ILs were fitted to the PR-EoS for $[C_4C_1im][PF_6]$, as shown in Figure 1, by adjusting parameters k_{ij} and l_{ij} with the goal of using the minimum number of binary parameters while minimizing error (<10% AARD). The PR-EoS has nine parameters to fit each binary system where $k_{ij} = k_{ji}$ and $l_{ij} \neq l_{ji}$.

model to real applications. The three types of efficiency applied to column performance are: (1) overall efficiency (analysis comparing the theoretical stages with the actual stages), (2) the Murphree efficiency (single plate analysis of the vapor and liquid equilibrium), and (3) local efficiency (single plate analysis of the VLE). To accurately determine these efficiencies, experimental data are required, otherwise predictions can be made with some uncertainty in the calculations.

3.2. Rate-Based (Non-Equilibrium) Model. Rate-based models, also known as non-equilibrium models, for distillation were first proposed in 1982.⁷⁹ These models have grown in popularity for various column internals, reactive distillations, and absorption systems and can predict the column profile without the need for estimating column or tray efficiencies. The column performance is calculated using rate equations and transfer coefficients for the mass and energy transfer through the gas-liquid interface instead of assuming each tray or stage is at equilibrium. The gas-liquid interface occurs on a surface

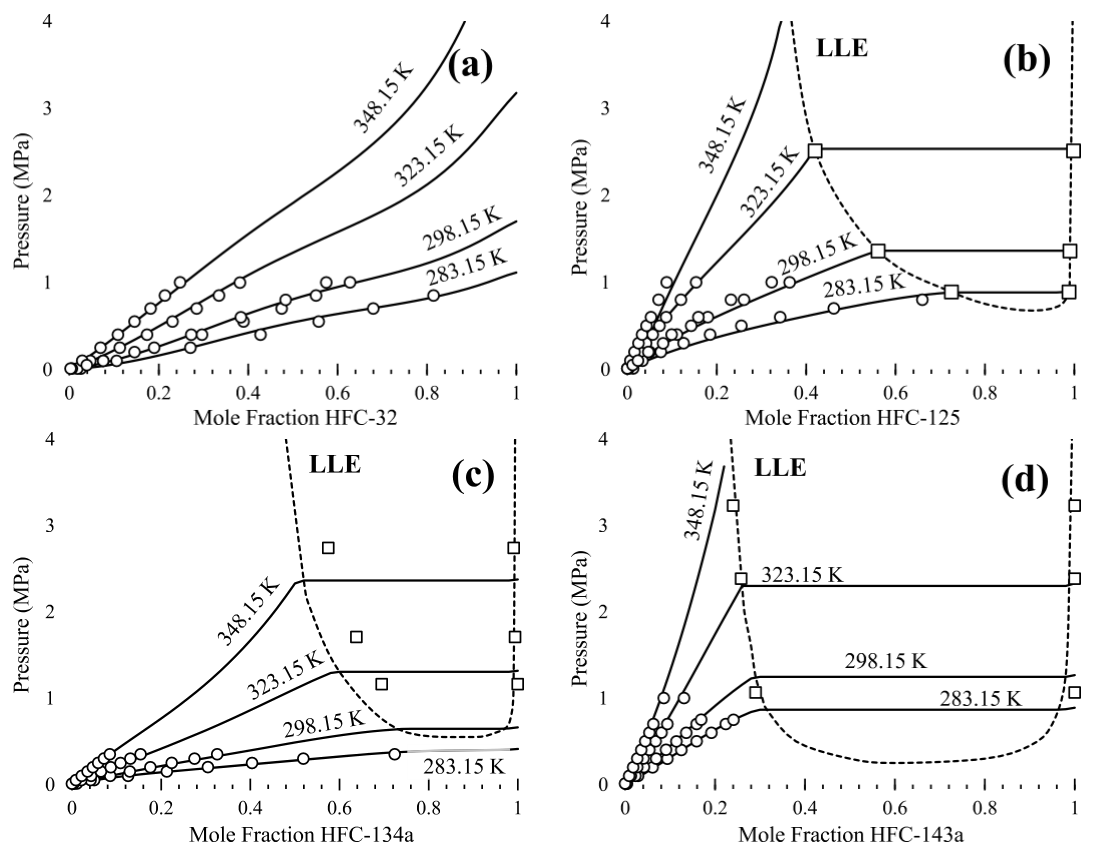


Figure 1. PTx data (\circ) for HFC-32 (a), HFC-125 (b), HFC-134a (c), and HFC-143a (d) with $[C_4C_1\text{im}][PF_6]^{56}$ and corresponding LLE data (\square) for HFC-125, ⁷³ HFC-134a, ⁷⁴ and HFC-143a. ⁷⁴

Table 3. Physical Properties for [C₂C₁im][Tf₂N] and [C₄C₁im][PF₆]

	property	temp. range (K)	correlation	C_1	C_2	<i>C</i> ₃	refs
$[C_2C_1im][Tf_2N]$	ρ (kg m ⁻³)	293.2 to 473.2	$z = C_1 + C_2 T$	1816.5	-0.9920		88^{b}
	μ (mPa s)	272.2 to 323.2	$\ln z = C_1 + C_2/T + C_3 \ln T$	-138.10	9054.9	19.52	58
	$C_{P,L}$ (J K ⁻¹ mol ⁻¹)	256.9 to 370.0	$z = C_1 + C_2T + C_3T_2$	362.96	0.4793	-1.544 ×	89^{b}
						10-6	88
	σ (mN m ⁻¹)	313.0 to 413.1	$z = C_1 + C_2 T$	51.130	-0.0514		а
	μ (mPa s)	288.2 to 313.2	$z = C_1 \exp(C_2/T) + C_3$	5.271×10^{-6}	5228.5	0	59
	$C_{P,L}$ (J K ⁻¹ mol ⁻¹)	283.2 to 550.0	$z = C_1 + C_2T + C_3T_2$	124.44	1.2403	-9.612×10^{-4}	90^b
	σ (mN m ⁻¹)	288.2 to 313.2	$z = C_1 + C_2 T$	63.552	-0.06773		91,
							92^{b}

aGeneralized equation provided by the NIST Database in ASPEN. bExperimental data regressed in this work.

(tray or packing) where the bulk liquid is flowing down the surface and bulk vapor is flowing up past the surface. Unlike the MESH equations, the rate-based model uses balances in the gas and liquid phases separately and considers mass and heat transfer resistances according to film theory by explicit calculation of interfacial fluxes and film discretization, accounting for the concentration and temperature gradients in both phases.⁸⁰ The rate-based model also considers the geometry and sizing of the column internals (trays or packings) to determine the effective interfacial area, pressure drops, and flooding or phenomena. Rate-based models weeping multicomponent mass transfer theory have led to more realistic stage models rather than empirical efficiency factors when incorporating nonequilibrium effects.81

Similar to the equilibrium model in determining N_T , rate-

based models can also be used to determine the column geometry (i.e., the height, diameter, and packing surface area) needed for mass transfer to achieve the desired purity in the

D

outlet streams. Successful application of the rate-based method for a packed column distillation simulation depends on the appropriate choice of prediction methods for transport properties and the effective interfacial area for heat and mass transfer.⁸² Though rate-based models require more computational effort, the added degree of rigor is necessary for modeling separations of components with similar boiling points and highly non-ideal separation processes.

The higher viscosities of ILs, compared to traditional organic solvent entrainers, can decrease the mass transfer efficiency, leading to the rate-based calculations and the equilibrium of the system to be a less effective prediction for column sizing.83,84 In 2013, Quijada-Maldonado et al.85 validated the accuracy of rate-based models with a pilot scale extractive distillation column using an IL entrainer and 750Y Mellapak Sulzer structured packing to separate ethanol and water. The IL entrainer 1-ethyl-3-methylimidazolium dicyanamide ([C2C1im][DCA]) was compared with the commonly used

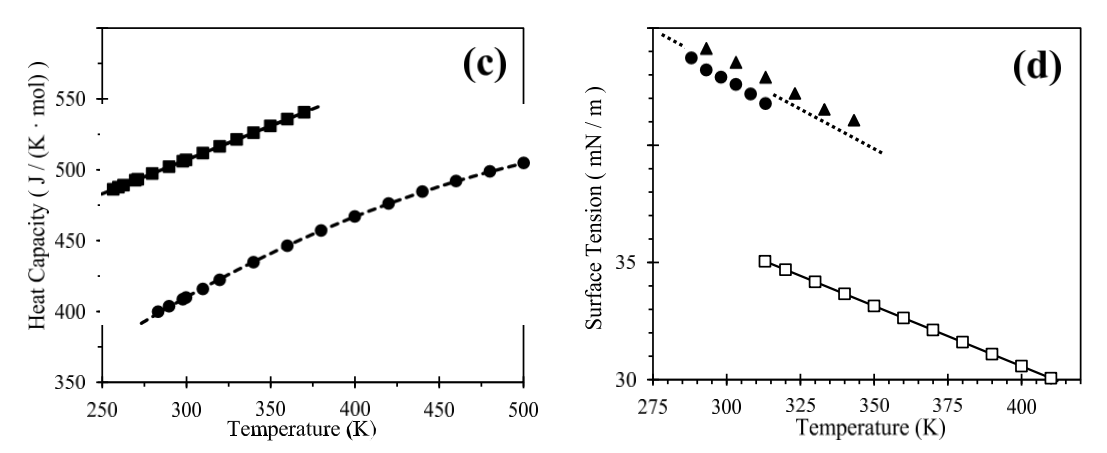


Figure 2. Physical properties for ILs. Viscosity (a), density (b), heat capacity (c), and surface tension (d) for $[C_2C_1\text{im}][Tf_2N]$ (\square) and $[C_4C_1\text{im}][PF_6]$ (\bigcirc , \triangle) shown in Table 3. Open symbols are plotted points from the correlation and the solid symbols are experimental data points from literature that were then regressed in this work.

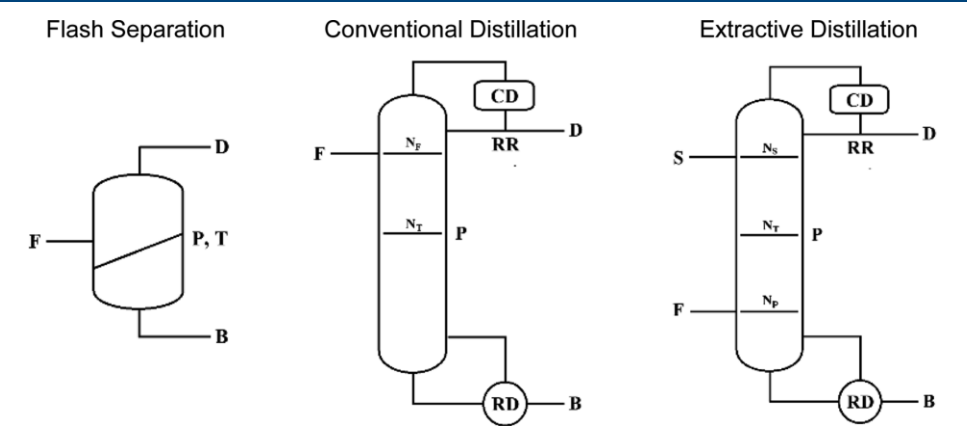
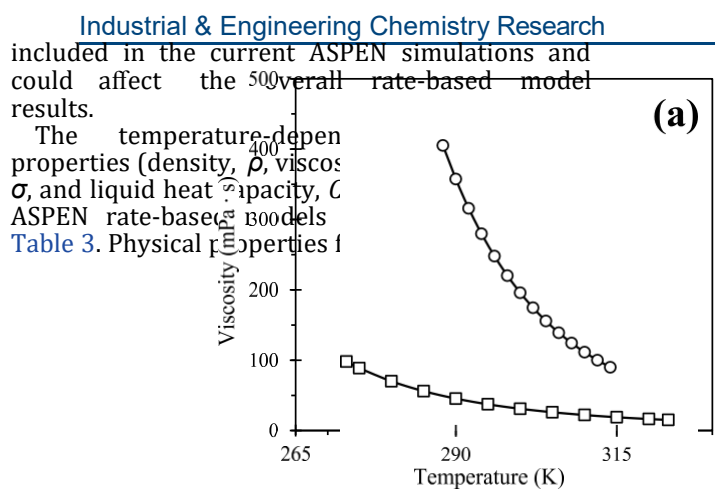


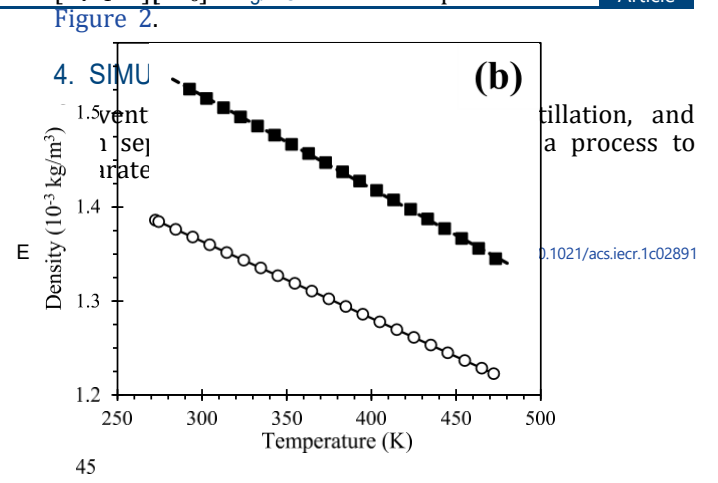
Figure 3. Separation methods, feed (F), bottoms (B), distillate (D), pressure (P), temperature (T), reboiler duty (RD), condenser duty (CD), reflux ratio (RR), feed stage (N_F), solvent stage (N_S), and total number of stages (N_T).

organic solvent entrainer, ethylene glycol (EG). Model prediction for the temperature profiles of both entrainers were compared at various solvent-to-feed ratios and distillate flowrates. Rocha, Bravo, and Fair's 86,87 rate-based model provided the best prediction for the pilot scale extractive distillation with a 10% total deviation from experimental data. The [C2C1im][DCA] achieved higher mass transfer efficiencies than EG over the range of solvent-to-feed ratios tested. It is important to note that the Quijada-Maldonado et al. simulation used experimental binary

and ternary mixture data for the density, viscosity, and surface tension that were not



600



refrigerant mixtures (R-404A, R-407C, R-410A, and R-410A + HCFC-22). The variables for each of these processes are shown in Figure 3. For both distillation processes, structured packing was used for its higher efficiency compared with trays, thus reducing the overall height of the column. The methodology for each simulation began with testing the separation of the refrigerant mixture with a (1) flash vessel, followed by evaluating a (2) conventional distillation, and finally using an (3) extractive distillation.

The flash vessel is a single stage equilibrium separation dependent only on temperature, T, and pressure, P. The flash vessel T was varied from 0 to 135 °C and P from 0.01 to 1.0 MPa. Ideally, the preferred pressure should be close to 0.1 MPa (i.e., atmospheric pressure), and the temperature should be close to 20 °C (i.e., ambient temperatures) or to the feed temperature. If the flash vessel did not achieve the desired purity and recovery for each of the refrigerant components in either the bottom stream (i.e., liquid) or top stream (i.e., vapor), then conventional distillation was modeled. It was important to test the separation with one or two components leaving the distillate (or vapor stream) because two of the three components might be more volatile (i.e., light key

components) and could be separated from the heavy key component. Conventional and extractive distillation columns provide additional variables to optimize, such as reflux ratio and solvent-to-feed ratio.

4.1. Constraints and Heuristics. To efficiently optimize

multiple variables, a set of constraints were defined and heuristics were created. The first constraint considered was the height of the column. The maximum height of 15 m was based on the maximum height in the University of Kansas (KU) unit operations laboratory high-bay area where a pilot-scale extractive distillation column is under construction. The second constraint was the reboiler temperature: 15 °C < T_{Reboiler} < 135 °C. The lower temperature limit is to avoid the need for a temperature thermostat, and the upper temperature limit is to avoid IL decomposition. The most preferred case (Case 1) would have $T_{\text{Reboiler}} < 100$ $^{\circ}$ C and the condenser temperature, $T_{\text{Condenser}} > 15 \, ^{\circ}$ C so that the chilled water supply in the KU unit operations laboratory can be used without the need for a lowtemperature thermostat. Case 2 would have the same $T_{\text{Reboiler}} < 100$ °C, but $T_{\text{Condenser}} > 0$ °C requiring a lowtemperature thermostat. If neither of these cases achieve the desired refrigerant purity, then Case 3 includes T_{Reboiler} < 135 °C. These temperature constraints are a function of the column operating pressure and the solvent-to-feed ratio.

A consistent heuristic in most simulations is that a liquidphase refrigerant feed will result in a higher distillate purity,

compared to a vapor-phase feed. In addition, the colder the refrigerant feed and solvent feed, the higher the distillate purity; therefore, the feeds were set at 20 °C (ambient temperature), so no additional cooling of the streams was necessary. Another heuristic included the IL feed always entering at the top of the packing, $N_S = 2$, because the IL has essentially no measurable vapor pressure. Other simulations referenced in introduction follow the same approaches.^{27–49}

To achieve complete separation of each component, the distillate rate, D, should equal either the mass fraction of one component multiplied by the feed (D = $z_i F$) resulting in the component leaving the distillate, or the mass fraction sum of the other components resulting in the component leaving the bottoms. This guided whether the separation was performed with one or two components of the ternary mixture in the distillate.

The present simulations used a feed rate, F = 10 kg/h, which is a recommended flow rate for a 10 cm diameter column using 750Y Mellapak Sulzer-structured packing (the highest surface area packing for pilot scale operation).93 The ASPEN rate- based model takes into consideration the volume of the structure packing and with a fixed column diameter, calculates the column height. The remaining variables to optimize included the pressure, P, feed stage, N_F, reflux ratio, RR, solventto-feed ratio, S/F, and the number of theoretical stages. $N_{\rm T}$, for the equilibrium model or height of packing for the rate- based model.

4.2. Optimizing Distillation. Optimizing P, N_F, RR, S/F (for extractive distillation), and N_T or height of packing can be challenging since some of the optimal values for each variable are dependent on each other. The data analysis showed that

(1) S/F, P, and N_T influenced the optimal N_F , while RR had a very small effect, (2) P was constrained by the resulting T_{Reboiler} and $T_{\text{Condenser}}$, so N_{T} could be increased or decreased at various P, (3) P determined the solubility of the refrigerant in the IL depending on the amount of solvent in the column, and (4), RR was the final adjustable variable for optimizing the distillate purity. The order in which the variables were optimized were $S/F \rightarrow P \rightarrow N_T \rightarrow N_F \rightarrow RR$. The optimization algorithm is shown in Figure 4.

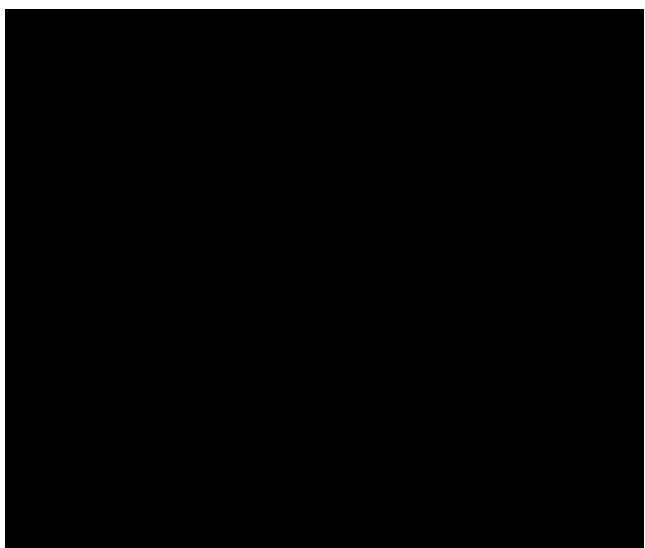


Figure 4. Diagram for optimizing distillate and bottoms purity using extractive distillation.

multiplied by the feed $(D = (1 - z_i)F)$

In Figuladustial & Engineering albentistry Research by the solid lines and extractive distillation, which requires an additional set of variables when introducing an IL entrainer, is represented by the dashed lines. If the desired purity cannot be achieved within the constraints of conventional distillation (i.e., azeotrope or closeboiling components), then extractive distillation will be considered for separation. If adding an IL solvent for extractive distillation did not result in the desired purity below a S/F = 20, then a different IL entrainer was considered. In the current study, $[C_2C_1][Tf_2N]$ was the first entrainer considered and [C₄C₁im][PF₆] was the second choice evaluated. Once the desired separation was achieved,

G

the next step was to repeat the optimization process by adjusting P to achieve the specified temperature constraints (i.e., cases 1, 2, or 3) and minimize the reboiler heat duty. If the unit operation was an extractive distillation column, then the next step was to repeat the process by decreasing the S/F ratio. Variables P and S/F ratio had the greatest impact on the heat duty. The final step repeated the process by decreasing the N_T or height of the packing.

A sensitivity analysis found that when separating one refrigerant from a ternary mixture using conventional distillation that the lower the operating pressure the fewer theoretical stages required (i.e., packing height); however, the reboiler and condenser temperatures also decrease and can become very cold (sub-ambient). For example, lowering the pressure when separating HFC-134a from HFC-32 and HFC- 125 in R-407C using conventional distillation can significantly increase the HFC-134a purity at $N_{\rm T}=20$ but will also decrease $T_{\rm Reboiler}$ as shown in Figure 5a. To remain within the temperature constraint of $T_{\rm Reboiler} > 15$ °C the lowest operating pressure for maximizing the purity of HFC-134a was between

0.4 and 0.6 MPa; however, this achieved a maximum distillate purity of only 99 wt % HFC-134a. To reach the specified HFC-134a purity of >99.5 wt %, the RR was optimized followed by $N_{\rm T}$ (or the packing height for the rate-based model) and the algorithm repeated.

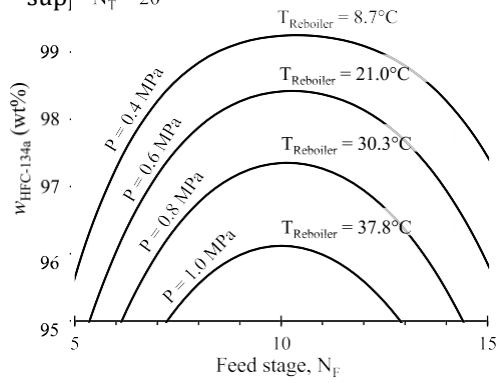
For extractive distillation, the opposite trend was found with pressure. Higher pressures required fewer theoretical stages or packing height to achieve the desired refrigerant purity. Increasing the pressure increased the refrigerant solubility in the IL entrainer, but also increased the T_{Reboiler} . For example, increasing the pressure when separating HFC-125 from HFC-32 and HFC-134a in R-407C using extractive distillation significantly increased the HFC-125 purity at $N_T = 20$, but also increased $T_{Reboiler}$ as shown in Figure 5b. There was a large increase in HFC-125 purity when raising the pressure from 0.8 to 1.0 MPa, but further pressure increases provided smaller improvements in purity with a maximum purity of about 99.4 wt % HFC-125 at $N_{\rm T}$ = 20 and 1.6 MPa. To increase HFC-125 purity to >99.5 wt %, the RR was adjusted, and if further increases were required, the $N_{\rm T}$ (or packing height) or S/F was increased. The initial values specified for optimizing the separation processes in Section 5 were: P = 8, $N_{\rm T} = 20$ (or packing height = 10 m), $N_{\rm F} = 10$, RR = 2, and, for extractive distillation, S/F = 5.

In the case of a commercial column, the capital versus operating costs would be considered to determine the lowest overall cost (operating and capital); this can be conducted by increasing the column height, which would increase product purity, avoiding the need to increase the S/F ratio and reduce the overall heat duty. For the current situation with a limited height of 15 m for constructing the pilot-scale column, our goal was to optimize columns *P*, S/F, and RR.

5. RESULTS

Refrigerant mixtures, R-404A, R-407C, R-410A, and R-410A with HCFC-22, were simulated using an equilibrium model and the Rocha et al. rate-based model with the goal of achieving 99.5 wt % purity for each component. The initial hypothesis assumed that the optimized parameters for each unit operation in the equilibrium model would be significantly different than the rate-based model; however, the equilibrium

and rate-based models provided similar optimal values for S/F ratio, P, $N_{\rm F}/N_{\rm T}$, and RR. This result $\sup_{t \to \infty} \sum_{t \to \infty} N_{\rm T} = 20$



100

WHFC-125 (Mt%)
80
90

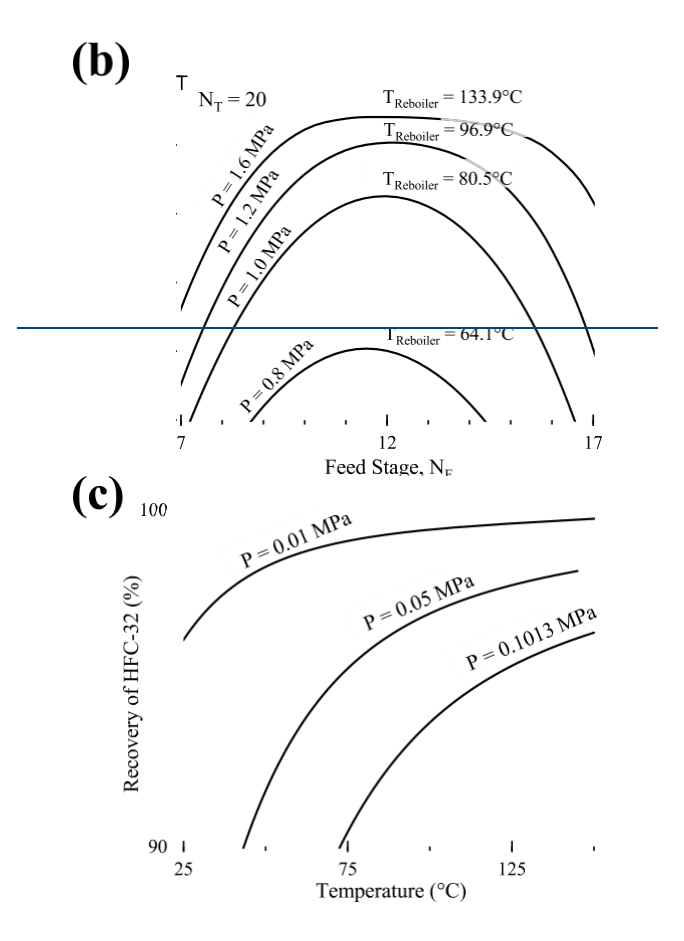
95

Figure 5. (a) Sensitivity analysis for $N_{\rm F}$ as a function of P at $N_{\rm T}=20$ for calculating HFC-134a bottoms purity using conventional distillation to separate R-407C. Condenser temperatures range from

-20.1 to 7.5 °C. (b) Sensitivity analysis for $N_{\rm F}$ as a function of P at $N_{\rm T}=20$ for calculating HFC-125 distillate purity using extractive distillation to separate R-407C. Condenser temperatures ranged from

4.5 to 30.0 °C. (c) Sensitivity analysis using a flash vessel for recovery of HFC-32 as a function of T and P.

benefit of rate-based models is to predict the number of actual trays or the height of structured packing needed for non-ideal systems. The results of the process flow diagrams (PFD) are shown in Figure 6a–d and are based on the rate-based model simulation and also provide the $N_{\rm T}$ found in the corresponding equilibrium model. The PFDs include the results for mass fractions, w_i , mass flow rates (F, S, B_n , and D_n), heat duties (Q), T, P, RR, feed locations ($N_{\rm S}$ and $N_{\rm F}$), packing height for 750Y



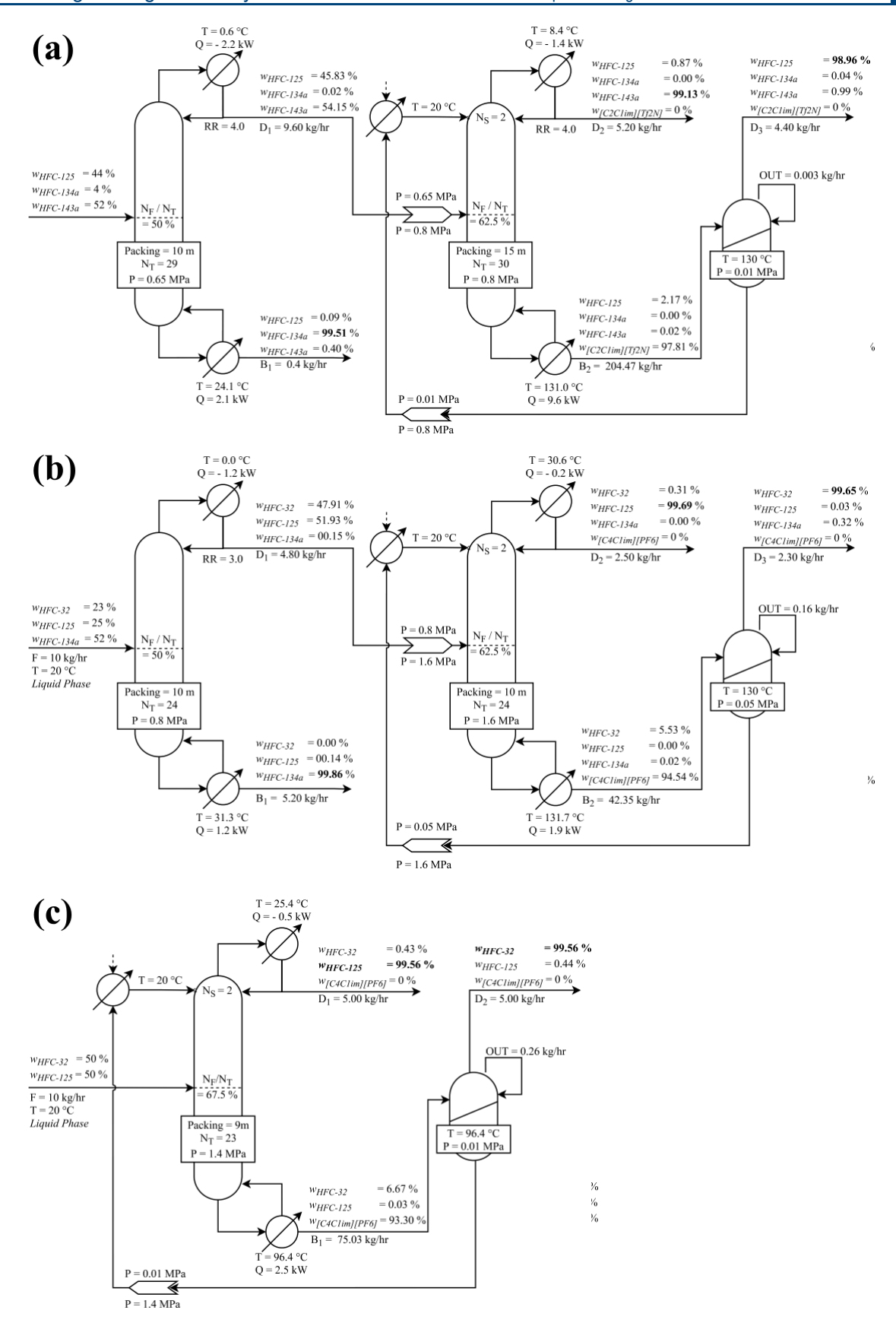


Figure 6. continued

https://doi.org/10.1021/acs.iecr.1c02891

Н

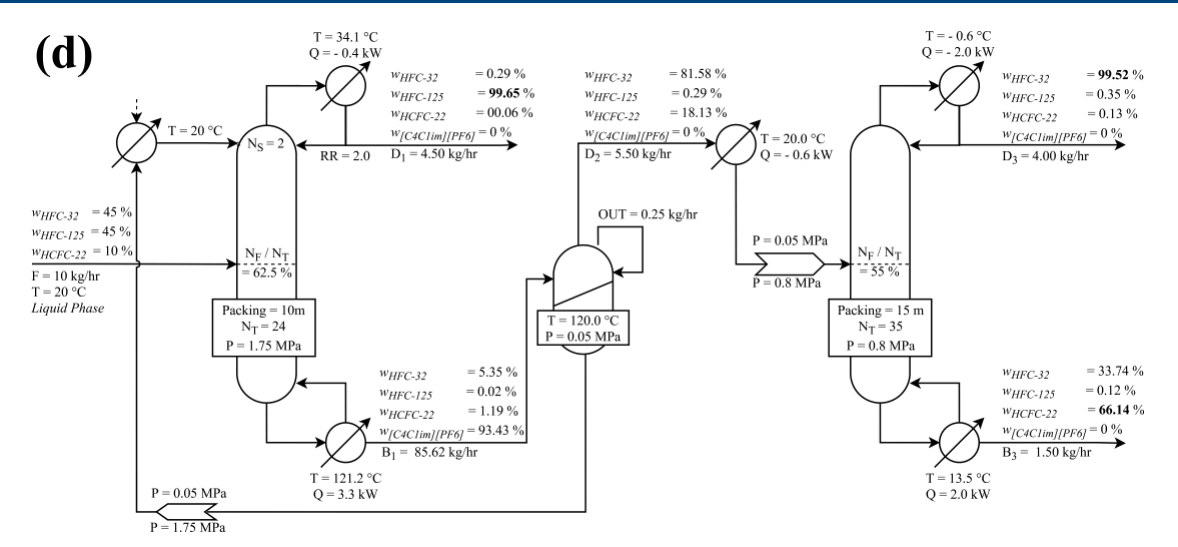


Figure 6. (a) Process for separating ternary refrigerant mixture R-404A with entrainer $[C_2C_1\text{im}][Tf_2N]$. (b) Process for separating ternary refrigerant mixture R-407C with entrainer $[C_4C_1\text{im}][PF_6]$. (c) Process for separating binary refrigerant mixture R-410A with entrainer $[C_4C_1\text{im}][PF_6]$. (d) Process for separating ternary refrigerant mixture R-410A with HCFC-22 and entrainer $[C_4C_1\text{im}][PF_6]$.

Mellapak Sulzer with a 10 cm diameter, and the theoretical stages from the equilibrium model, N_T .

Two options were considered for recovering the ionic liquid after the extractive distillation using a flash vessel and a stripping column. Because the ILs are nonvolatile, recovering the solvent using a single stage flash separation was found to be optimal. The stripping column resulted in a higher energy input and higher reboiler temperatures. The flash vessel did require vacuum operation, but overall the energy required was the lowest of the two options. A sensitivity analysis for the separation of HFC-32 from R-407C using a flash vessel as a function of T and P is shown in Figure 5c. Atmospheric pressure was not low enough to fully recover HFC-32; therefore, a vacuum was required. The small amount of refrigerant ($w_{ref} < 0.5$ wt %) remaining in the recycled IL aided in decreasing the viscosity of the fluid and reducing pumping power; however, this amount had to be balanced with the purity required in the distillate from the extraction distillation column. In the vapor stream from the flash vessel, there was a trace amount of IL (defined as the "OUT" stream). The PR- EoS slightly overpredicted the vapor pressure for the IL which accounts for this loss. An outlet was added to the flash tank to account for this loss that was recycled back to the column (similar to how a demister would be used if ionic liquid were entrained in the vapor, see Figure 6a-d).

5.1. Separation R-404A. The PFD for separating R-404A

is shown in Figure 6a. HFC-134a has a higher relative volatility and boiling temperature compared with HFC-125 and HFC- 143a. Separation was achieved using conventional distillation by removing HFC-125 and HFC-143a in the distillate and collecting HFC-134a from the bottoms of the first conventional distillation column. The optimal pressure for separating these HFC refrigerants was about 0.3 MPa, but the pressure was set at a minimum of 0.65 MPa to remain within the constraint of Case 2 ($T_{\rm Condenser} > 0$ °C). A bottoms composition of 99.5 wt % HFC-134a was achieved with $N_{\rm T}$

= 29 and a packing height of 10 m. Impurities included 0.4 wt

% HFC-143a and 0.1 wt % HFC-125.

HFC-125 and HFC-143a from the distillate could not be separated with conventional distillation as expected because these HFCs form an azeotrope at 46.3 wt % HFC-125 and 53.7

Industrial & Engineering Chemistry Research wt % HFC-143a at -46.7 °C.52,94 Extractive distillation was used with IL $[C_2C_1im][Tf_2N]$ as the entrainer. The maximum constraints for the S/F ratio of 20, packing height of 15 m, and pressure of 0.8 MPa were required to maintain a $T_{\text{Reboiler}} < 135$

°C. Prior to connecting the recycle stream, increasing RR decreased the distillate purity, which was not expected, but is the result of HFC-143a returning to the rectifying section (i.e., azeotropic section) of the column. Also, increasing the amount of HFC-143 returning to the column in the IL reduced the separation efficiency. The addition of the IL recycle stream and increasing the RR to 4.0 led to a slight increase in the distillate purity within the constraints specified.

The HFC-143a composition in the distillate was about 99.1 wt % with 0.9 wt % HFC-125. The HFC-125 absorbed in the IL exited the bottom of the column. The HFC-125 was separated from the IL entrainer using a flash vessel operating under a vacuum of P = 0.01 MPa and T = 130 °C. The purity of HFC-125 obtained was about 99.0 wt % with 1.0 wt % HFC-143a.

Increasing the pressure above 0.8 MPa increased

the refrigerant pyrities, but also increased the repoiler temperature of the extractive distillation column beyond the constraints specified in Cases 1-3. Increasing the packing height also resulted in a higher purity. Higher pressures (up to 2.0 MPa) and a taller column (up to 50 m) were modeled to determine if >99.5 wt % HFC-143a and HFC-125 purities could be achieved. The highest HFC-143a purity of 99.5 wt % and the highest HFC-125 purity of 99.4 wt % were achieved at 1.1 MPa and 30 m. The separation process was repeated with $[C_4C_1im][PF_6]$ as the entrainer and the maximum HFC-143a was about 83.9 wt %, and the HFC-125 was about 81.0 wt % (see Figure S4 in the Supporting Information). HFC-125 and HFC-143a also have LLE (see Figure 1b,d) that needs to be carefully considered when operating the extractive distillation column and flash separation vessel.

5.2. Separation R-407C. The PFD for separating R-407C is shown in Figure 6b. Similar to the separation of R-404A, HFC-134a has a higher relative volatility and boiling temperature than the other two components (HFC-32 and HFC-125). Separation was achieved using conventional distillation by boiling off HFC-32 and HFC-125 and collecting

Ī

HFC-134a from the bottoms. To achieve the necessary purity of HFC-134a, the pressure was set at 0.8 MPa to satisfy $T_{\rm Condenser} > 0$ °C (constraint Case 2). A bottom composition of

99.9 wt % HFC-134a was achieved with 0.1 wt % HFC-125 with N_T = 24 and a packing height of 10 m.

HFC-32 and HFC-125 form an azeotrope at 67.8 wt % HFC-32 and 32.2 wt % HFC-125 at -52.1 °C,^{52,95} and

extractive distillation with an entrainer was required for The initial ASPEN model using [C C

achieved a distillate purity of 95.9 wt % HFC-125 and 95.6 wt

% HFC-32 with the constraints specified in Cases 1–3 (see Figure S5 in the Supporting Information). Because >99.5 wt % purity was not achieved, the simulation was repeated using $[C_4C_1im][PF_6]$ as the entrainer.

A purity of 99.7 wt % HFC-125 with 0.3 wt % HFC-32 was achieved at a S/F ratio of 8 and a packing height of 10 m or N_T

- = 24. The pressure was set at 1.6 MPa to keep the reboiler temperature ($T_{\rm Reboiler}$ < 135 °C) within the constraint of Case
- 3. The system could be further optimized to reduce $T_{\rm Reboiler}$ and $Q_{\rm Reboiler}$ by decreasing the P or S/F ratio and increasing the packing height. The HFC-32 absorbed in the IL exits the bottoms stream and is fed into a flash vessel at a vacuum of P =

0.05 MPa and T = 130 °C, where the HFC-32 desorbs from

the IL. The vapor stream of the flash vessel achieved 99.7 wt % HFC-32 with 0.3 wt % HFC-134a, and the IL recycled back to the extractive distillation column contained about 0.13 wt % HFC-32.

5.3. Separation R-410A. The PFD for separating R-410A

is shown in Figure 6c. The mixture of HFC-32 and HFC-125 forms an azeotrope and cannot be separated with conventional distillation; therefore, extractive distillation is required. The initial separation using [C₂C₁im][Tf₂N] as the entrainer achieved a maximum purity of 95.5 wt % of HFC-125 in the distillate and 95.5 wt % HFC-32 in the vapor stream of the flash vessel with the constraints specified in Cases 1-3 (see Figure S6 in the Supporting Information). This confirms from the separation of R-407C that $[C_2C_1im][Tf_2N]$ is not an adequate solvent to separate the azeotropic mixture HFC-32 + HFC-125. Next, the separation was simulated with $[C_4C_1im]$ - $[PF_6]$, the more selective solvent for HFC-125 versus HFC-32, and achieved a distillate composition of 99.6 wt % HFC-125 with 0.4 wt % HFC-32. The system was operated with the most preferred reboiler and condenser temperatures for Case

1. A sensitivity analysis was performed with a packing height of 9 m for different S/F ratios and pressures. A column pressure of P=1.4 MPa and S/F = 7 achieved a distillate purity >99.5 wt % HFC-125 at a minimum $Q_{\rm Reboiler}=2.5$ kW. The bottoms of the extractive distillation column was fed to a flash vessel operating at a vacuum of P=0.01 MPa and T=96.4 °C (equal to $T_{\rm Reboiler}$) where HFC-32 desorbed from the IL and the IL was recycled back to the extractive distillation column. The vapor stream of the flash vessel achieved 99.6 wt % HFC-32 with 0.4 wt % HFC-125, and the recycled IL contained a minimal amount of refrigerant (0.04 wt % HFC-32).

5.4. Separation K-410A with HCFC-22. The PFD

form an azeotrope, but the mixture is near-azeotropic and difficult to separate.

Conventional distillation was modeled for separation of R- 410A and HCFC-22, but the maximum bottom purity was 72 wt % HCFC-22 with trace amounts of HCFC-22 in the distillate. Extractive distillation was modeled using [C_2C_1 im]- [Tf_2N] as the entrainer, but only reached a maximum purity of

87.2 wt % HFC-125 in the distillate with the constraints

for

separating R-410A with HCFC-22 is shown in Figure 6d. HFC-32, HFC-125, and HCFC-22 all have similar normal boiling points (-51.65, -48.09, -40.81 °C, respectively).⁵¹ In addition, binary mixtures HFC-32 + HFC-125 and HCFC-22 + HFC-125 form azeotropes. The HCFC-22 + HFC-125 form an azeotrope at approximately 5 wt % HCFC-22 and 95 wt % HFC-125 at -48.1 °C (see Figure S7 in the Supporting Information). Binary mixture HFC-32 + HCFC-22 does not

pubs.acs.org/IECR

repeated using $[C_4C_1im][PF_6]$ as the entrainer. A distillate purity of 99.5 wt % HFC-125, 0.3 wt % HFC-32, and 0.1 wt % HCFC-22 was achieved within the temperature constraints of Case 3 at a column pressure of 1.4 MPa. When pressure was increased to achieve an even higher purity, this resulted in a reboiler temperature that no longer satisfied Case 3 ($T_{Reboiler}$ < 135 °C). The bottoms of the extractive distillation column was fed

to a flash vessel operating at a vacuum of P = 0.05 MPa and

= 120 °C. HFC-32 and HCFC-22 were desorbed from the IL and the IL containing 0.12 wt % HFC-32, and 0.03 wt % HCFC-22 was recycled back to the extractive distillation column.

The refrigerant stream containing primarily HFC-32 and HCFC-22 from the flash vessel was condensed to a liquid at ambient temperature (T =20 °C) and fed to a conventional distillation column. Even though HFC-32 and HCFC-22 do not form an azeotrope, conventional distillation was not effective at separating these refrigerants to a purity of >99.5 wt

% within the constraints provided in Cases 1-3; therefore.

extractive distillation is recommended to increase the relative volatilities of the components. The solubility of HFC-32 and HCFC-22 are both high in the modeled entrainers [C₂C₁im]- [Tf₂N] and $[C_4C_1im][PF_6]$ resulting in low selectivity; therefore, a new entrainer should be identified. For this reason, conventional distillation was modeled to determine the maximum amount of HFC-32 that can be recovered from HCFC-22 within the constraints specified. The distillate contained 98.5 wt % HFC-32 at the maximum distillate rate of D = 4.5 kg/h, and the bottoms contained 94.4 wt % HCFC-

22. The distillate rate has the largest effect on purity, but changes the total amount of refrigerant recovery. To increase the HFC-32 purity in the distillate, the distillate rate of D = 4.5 kg/h was decreased, but this also decreased the purity of HCFC-22 leaving the bottoms and the percent recovery of HFC-32.

A distillate purity of 99.5 wt % HFC-32, 0.4 wt % HFC-125, and 0.1 wt % HCFC-22 was achieved at D = 4.0 kg/h (about 90% recovery of the HFC-32), and the bottoms contained 66.1 wt % HCFC-22, 33.7 wt % HFC-32, and 0.1 wt % HFC-125 as shown in Figure 6d. In this case, approximately 0.50 kg/h (about 10%) of the HFC-32 was not recovered from the bottom. To recover additional HFC-32, more work on new entrainers with higher selectivity is recommended.

Additional simulations were conducted outside the current constraints (Cases 1 to 3) to determine the highest purity that could be achieved for both HFC-32 and HCFC-22 using conventional distillation. A distillate composition of 99.5 wt % HFC-32 at a D = 4.5 kg/h and a bottom purity of 99.5 wt % HCFC-22 was possible with a packing height of 54 m and an operating pressure of 2 bar, resulting in reboiler and condenser temperatures of $T_{\text{Reboiler}} = -25.3$ °C and $T_{\text{Condenser}} = -37.1$ °C.

6. CONCLUSIONS

Many commercial refrigerant mixtures such as R-404A, R- 407C, and R-410A contain components that form azeotropic mixtures. Some components of these mixtures, such as HFC- 32, can be separated and reused to prepare new low-GWP mixtures with HFO refrigerants. Separation of refrigerants, particularly, ozone depleting chemicals such as HCFC-22, will reduce the amount of HFCs that have to be incinerated, which otherwise could be recycled. Distillation is a common process for separating refrigerant mixtures; however, if azeotropes are present, complete separation of the components is not possible. Extractive distillation is a common technology used to separate azeotropic mixtures or close boiling point solvents with the use of an entrainer to alter the liquid phase properties and to modify the volatility of each component for more efficient separation. For HFC separations, ILs have been shown to be good candidates as entrainers for extractive distillation. ILs have negligible vapor pressure that reduces losses in the distillate and are chemically stable over a wide temperature range needed for reboiler operation. In this work, simulations are provided for the separation of R-404A, R- 407C, R-410A, and R-410A + HCFC-22 with two IL entrainers ($[C_2C_1im][Tf_2N]$ and $[C_4C_1im][PF_6]$). Equilibrium and rate-based models using the PR-EoS were used for the ASPEN simulations, and HFC + IL VLE data were fit within 10% AARD over the entire composition range.

The R-404A separation scheme was able to achieve 99.5 wt

% purity for the HFC-134a using conventional distillation but was not able to achieve the same purity for separating the azeotropic mixture of HFC-125 and HFC-143a using extractive distillation and entrainers $[C_2C_1\mathrm{im}][Tf_2N]$ and $[C_4C_1\mathrm{im}][PF_6]$ within the constraints specified in Cases 1–3. The highest purity achieved in the distillate for HFC-143a was

99.1 wt % at the maximum packing height, RR, and S/F ratio. Additional simulations were run at higher pressures and packing heights beyond the constraints specified that achieved a maximized purity of 99.5 wt % HFC-143a and 99.4 wt % HFC-125.

The R-407C separation scheme was able to achieve 99.9 wt

% HFC-134a purity with a conventional distillation column and 99.7 wt % purity for both HFC-125 and HFC-32 using an extractive distillation column and the $[C_4C_1\mathrm{im}][PF_6]$ ionic liquid entrainer. The separation of the azeotropic mixture HFC-32 and HFC-125 was not able to achieve a purity greater than 95.9 wt % HFC-125 using the $[C_2C_1\mathrm{im}][Tf_2N]$ ionic liquid entrainer within the constraints specified.

The R-410A separation scheme was able to achieve 99.6 wt

% purity for both HFC-125 and HFC-32 using an extractive distillation column and the [C_4C_1 im][PF6] ionic liquid entrainer. Similar to the R-407C separation, the [C_2C_1 im]- [Tf2N] ionic liquid entrainer could only achieve 95.5 wt % HFC-125 purity in the distillate within the constraints specified.

A separation scheme was also modeled for a mixture containing R-410A and 10 wt % HCFC-22 to determine what purities could be achieved and how much HFC-32 can be recovered. Purities of 99.5 and 99.7 wt % were achieved for HFC-32 and HFC-125, respectively. In addition, about 90 and 99.7% of HFC-32 and HFC-125

was recovered. Separation of HCFC-22 and HFC-32 was challenging because these components have similar boiling points. Conventional distillation did achieve separation of these two components

Article

but required a packing height of 54 m and very low $T_{\rm Condenser}$ and $T_{\rm Reboiler}$; in this case, extractive distillation with a selective solvent between HFC-32 and HCFC-22 would be beneficial. Overall, azeotropic refrigerant mixtures such as R-404A, R-407C, R-410A, and R-410A + HCFC-22 can be separated to refrigerant purities of about 99.5 wt % in most cases using the proper ionic liquid entrainers. Future work will focus on experimentally verifying these simulations using a pilot scale extractive distillation column that is currently under con-struction and modeling how to separate higher component refrigerant mixtures.

ASSOCIATED CONTENT

*Supporting Information

The Supporting Information is available free of charge at https://pubs.acs.org/doi/10.1021/acs.iecr.1c02891

Regressed ideal heat capacities for both ILs, regressed Peng–Robinson parameters to solubility data, PTx figures for HFC's in ionic liquid [C₄C₁im][PF₆], PTx figures for HCFC-22 in both ILs, additional process simulation and design results, and Txy data for HCFC-22 and HFC-125 to define azeotrope point(PDF)

AUTHOR INFORMATION

Corresponding Author

Mark B. Shiflett – Institute for Sustainable Engineering, University of Kansas, Lawrence, Kansas 66045, United States; Department of Chemical and Petroleum Engineering, University of Kansas, Lawrence, Kansas 66045, United States; orcid.org/0000-0002-8934-6192; Email: Mark.B.Shiflett@ku.edu

Author

Ethan A. Finberg – Institute for Sustainable
Engineering, University of Kansas, Lawrence,
Kansas 66045, United States; Department of
Chemical and Petroleum Engineering, University of
Kansas Lawrence, Kansas 66045, United States;
orcid.org/0000-0002-4702-016X

Complete contact information is available at: https://pubs.acs.org/10.1021/acs.iecr.1c02891

Notes

The authors declare no competing financial interest.



The authors would like to acknowledge Ngan Tran, Senior Chemical Engineering undergraduate researcher, for conduct- ing the literature review on physical properties of ionic liquids and alternative entrainers. The authors would also like to acknowledge Dr. Alejandro Garciadiego Del Rio, a post- doctoral researcher at the University of Notre Dame in the Department of Chemical and Biomolecular Engineering, who assisted with the ASPEN modeling. Finally, the authors would like to thank Dr. Luke Simoni at Chemours for the HCFC-22

+ HFC-125 Txy equilibrium data.

REFERENCES

(1) High-GWP Refrigerants California Air Resources Board. https:// ww2.arb.ca.gov/resources/documents/high-gwp-refrigerants (ac- cessed Sept 9, 2021).

(2) EU Legislation to Control F-Gases. https://ec.europa.eu/clima/ policies/f-gas/legislation_en (accessed Jun 14, 2021).

Κ

- (3) Montreal Protocol on Substances that Deplete the Ozone Layer.
- https://www.environment.gov.au/protection/ozone/montreal-protocol (accessed Jun 14, 2021).
- (4) Recent International Developments under the Montreal Protocol. https://www.epa.gov/ozone-layer-protection/recent-international-developments-undermontreal-protocol (accessed Jun 14, 2021).
- (5) AIM Act. https://www.epa.gov/climate-hfcs-reduction/aim-act (accessed Jun 14, 2021).
- (6) Booten, C.; Nicholson, S.; Mann, M.; Abdelaziz, O. *Refrigerants: Market Trends and Supply Chain Assessment*; Clean Energy Manufacturing Analysis Center: Golden, CO, 2020; p 65.
- (7) Bivens, D. B.; Shiflett, M. B.; Yokozeki, A. Near-Azeotropic
- Blends for Use as Refrigerants. U.S. Patent 5,277,834 A, 1994.
- (8) Shiflett, M. B. Constant Boiling Compositions of Pentafluoro- ethane, Difluoromethane, and Tetrafluoroethane. U.S. Patent 5,185,094 A, 1993.
- (9) Shiflett, M. B. Refrigeration Process Using Constant Boiling
- Compositions of HFC-32, HFC-125 and HFC-134a. U.S. Patent 5,709,092 A, 1996.
- (10) Shiflett, M. B. Constant Boiling Compositions of HFC-32,
- HFC-125 and HFC-134 A. U.S. Patent 5,643,492 A, 1996.
- (11) Drout, W. M. Extractive Distillation Process. U.S. Patent 2,610,141 A, 1952.
- (12) Doherty, M. F.; Malone, M. F. *Conceptual Design of Distillation Systems*, 1st ed.; McGraw-Hill Companies, Inc.: New York, KY, 2001; p 568.
 (13) Doherty, M. F.; Knapp, J. P. Distillation, Azeotropic, and
- (13) Doherty, M. F.; Knapp, J. P. Distillation, Azeotropic, and Extractive. *Kirk-Othmer Encyclopedia of Chemical Technology*; John Wiley & Sons, Inc., 2004; Vol. 8, pp 358–398.
- (14) Lei, Z.; Li, C.; Chen, B. Extractive Distillation: A Review. *Sep. Purif. Rev.* 2003, *32*, 121–213.
- (15) Lei, Z.; Dai, C.; Zhu, J.; Chen, B. Extractive Distillation with Ionic Liquids: A Review. *AIChE J.* 2014, *60*, 3312–3329.
- (16) Meindersma, G. W.; Quijada-Maldonado, E.; Jongmans, M. T. G.; Hernandez, J. P. G.; Schuur, B.; de Haan, A. B. Extractive Distillation with Ionic Liquids: Pilot Plant Experiments and Conceptual Process Design. *Ionic Liquids for Better Separation Processes*; Springer, 2015; Vol. 1, pp 11–38.
- (17) Werner, S.; Haumann, M.; Wasserscheid, P. Ionic Liquids in Chemical Engineering. *Annu. Rev. Chem. Biomol. Eng.* 2010, 1, 203–230.
- (18) Kazakov, A. F.; Magee, J. W.; Chirico, R. D.; Diky, V.; Kroenlein, K. G.; Muzny, C. D.; Frenkel, M. D. Ionic Liquids Database ILThermo (v2.0). https://ilthermo.boulder.nist.gov (accessed September 12, 2021).
- (19) Mellein, B. R.; Scurto, A. M.; Shiflett, M. B. Gas solubility in ionic liquids. *Curr. Opin. Green Sustainable Chem.* 2021, 28, 100425.
- (20) Shiflett, M. B.; Maginn, E. J. The Solubility of Gases in Ionic Liquids. *AIChE J.* 2017, *63*, 4722–4737.
- (21) Lei, Z.; Dai, C.; Chen, B. Gas Solubility in Ionic Liquids. *Chem. Rev.* 2013, 114, 1289–1326.
- (22) Pereiro, A. B.; Araujo, J. M. M.; Esperança J. M. S. S.;
- Marrucho, I. M.; Rebelo, L. P. N. Ionic liquids in separations of azeotropic systems A review. *J. Chem. Therm.* 2012, 46, 2–28
- (23) Arlt, W.; Seiler, M.; Jork, C.; Schneider, T. Ionic Liquids as Selective Additives for Separation of Close-Boiling or Azeotropic Mixtures. U.S. Patent 2004/0133058 A1, 2004.
- (24) Beste, Y. A.; Shoenmakers, H.; Arlt, W.; Seiler, M.; Jork, C. Recycling of Ionic Liquids Produced in Extractive Distillation. U.S. Patent 2006/0272934 A1, 2006.
- (25) Massonne, K. Ionic Liquids at BASF SE. http://www.wet.kuleuven.be/english/summerschools/ionicliquids/lectures/ma

ssonne. pdf (accessed March 3, 2020).

(26) Meindersma, G. W.; Quijada-Maldonado, E.; Aelmans, T. A. M.; Hernandez, J. P. G.; de Haan, A. B. Ionic Liquids in Extractive Distillation of Ethanol/Water: From Laboratory to Pilot Plant. In *Ionic Liquids: Science and Applications*; Visser, A. E., Bridges, N. J.,

- Rogers, R. D., Eds.; American Chemical Society: Washington, DC, 2012; Vol. 1117, pp 239–257.
- (27) Ayuso, M.; Canada-Barcala, A.; Larriba, M.; Navarro, P.; Delgado-Mellado, N.; García, J.; Rodríguez, F. Enhanced separation of benzene and cyclohexane by homogeneous extractive distillation using ionic liquids as entrainers. *Sep. Purif. Technol.* 2020, 240, 116583.
- (28) Ayuso, M.; Navarro, P.; Palma, A. M.; Larriba, M.; Delgado- Mellado, N.; García, J.; Rodríguez, F.; Coutinho, I. A. P.; Carvalho, P.
- J. Separation of benzene from methylcycloalkanes by extractive distillation with cyano-based ionic liquids: Experimental and CPA EoS modelling. *Sep. Purif. Technol.* 2020, *234*, 116128.
- (29) Navarro, P.; Ovejero-Pérez, A.; Ayuso, M.; Delgado-Mellado, N.; Larriba, M.; García, J.; Rodríguez, F. Cyclohexane/cyclohexene separation by extractive distillation with cyano-based ionic liquids. *J. Mol. Liq.* 2019, *289*, 111120.
- (30) Navarro, P.; Ayuso, M.; Palma, A. M.; Larriba, M.; Delgado- Mellado, N.; García, J.; Rodríguez, F.; Coutinho, J. A. P.; Carvalho, P.
- J. Toluene/n-Heptane Separation by Extractive Distillation with Tricyanomethanide-Based Ionic Liquids: Experimental and CPA EoS Modeling. *Ind. Eng. Chem. Res.* 2018, *57*, 14242–14253.
- (31) Navarro, P.; de Dios-García, I.; Larriba, M.; Delgado-Mellado, N.; Ayuso, M.; Moreno, D.; Palomar, J.; García, J.; Rodríguez, F. Dearomatization of pyrolysis gasoline by extractive distillation with 1- ethyl-3-methylimidazolium tricyanomethanide. *Fuel Process. Technol.* 2019, *195*, 106156.
- (32) Li, W.; Xu, B.; Lei, Z.; Dai, C. Separation of benzene and cyclohexane by extractive distillation intensified with ionic liquid. *Chem. Eng. Process: Process Intensif.* 2018, *126*, 81–89.
- (33) Díaz, I.; Palomar, J.; Rodríguez, M.; de Riva, J.; Ferro, V.; González, E. J. Ionic liquids as entrainers for the separation of aromatic-aliphatic hydrocarbon mixtures by extractive distillation. *Chem. Eng. Res. Des.* 2016, *115*, 382–393.
- (34) Zhu, Z.; Ri, Y.; Li, M.; Jia, H.; Wang, Y.; Wang, Y. Extractive distillation for ethanol dehydration using imidazolium-based ionic liquids as solvents. *Chem. Eng. Process: Process Intensif.* 2016, 109, 190–198.
- (35) Ramírez-Corona, N.; Ek, N.; Jiménez-Gutiérrez, A. A method for the design of distillation systems aided by ionic liquids. *Chem. Eng. Process: Process Intensif.* 2015, 87, 1–8.
- (36) Jaimes Figueroa, J. E.; Rodrigues, M. I.; Maciel, M. R. W. Sequential strategy of experimental design I: Optimization of extractive distillation process of ethanol-water using [bmim][N(CN)- 2] as entrainer. *Chem. Eng. Process: Process Intensif.* 2015, 93, 56–60.
- (37) Seiler, M.; Jork, C.; Kavarnou, A.; Arlt, W.; Hirsch, R. Separation of Azeotropic Mixtures Using Hyperbranched Polymers or Ionic Liquids. *AIChE J.* 2004, *50*, 2439–2454.
- (38) Alvarez, V. H.; Alijó, P.; Serrao, D.; Filho, R. M.; Aznar, M.; Mattedi, S. Production of Anhydrous Ethanol by Extractive Distillation of Diluted Alcoholic Solutions with Ionic Liquids. *Comput.-Aided Chem. Eng.* 2009, 27, 1137–1142.
- (39) Figueroa, J. J.; Lunelli, B. H.; Filho, R. M.; Maciel, M. R. W. Improvements on Anhydrous Ethanol Production by Extractive Distillation using Ionic Liquid as Solvent. *Procedia Eng.* 2012, *42*, 1016–1026.
- (40) Aniya, V.; De, D.; Satyavathi, B. Comprehensive Approach toward Dehydration of tert-Butyl Alcohol by Extractive Distillation: Entrainer Selection, Thermodynamic Modeling and Process Optimization. *Ind. Eng. Chem. Res.* 2016, *55*, 6982–6995.
- (41) Li, J.; Li, T.; Peng, C.; Liu, H. Extractive Distillation with Ionic Liquid Entrainers for the Separation of Acetonitrile and Water. *Ind. Eng. Chem. Res.* 2019, 58,

- 5602-5612.
- (42) Chen, H.-H.; Chen, M.-K.; Chen, B.-C.; Chien, I.-L. Critical Assessment of Using an Ionic Liquid as Entrainer via Extractive Distillation. *Ind. Eng. Chem. Res.* 2017, 56, 7768–7782.
- (43) Ma, S.; Shang, X.; Zhu, M.; Li, J.; Sun, L. Design, optimization and control of extractive distillation for the separation of isopropanol- water using ionic liquids. *Sep. Purif. Technol.* 2019, *209*, 833–850.
- (44) Wu, L.; Wu, L.; Liu, Y.; Guo, X.; Hu, Y.; Cao, R.; Pu, X.; Wang, X. Conceptual design for the extractive distillation of cyclopentane

- and neohexane using a mixture of N,N-dimethyl formamide and ionic liquid as the solvent. *Chem. Eng. Res. Des.* 2018, 129, 197–208.
- (45) Song, Z.; Li, X.; Chao, H.; Mo, F.; Zhou, T.; Cheng, H.; Chen, L.; Qi, Z. Computer-aided ionic liquid design for alkane/cycloalkane extractive distillation process. *Green Energy Environ.* 2019, *4*, 154–165
- (46) Zhu, Z.; Ri, Y.; Jia, H.; Li, X.; Wang, Y.; Wang, Y. Process evaluation on the separation of ethyl acetate and ethanol using extractive distillation with ionic liquid. *Sep. Purif. Technol.* 2017, 181, 44–52.
- (47) Zhu, Z.; Hu, J.; Geng, X.; Qin, B.; Ma, K.; Wang, Y.; Gao, I.
- Process design of carbon dioxide and ethane separation using ionic liquid by extractive distillation. *J. Chem. Technol. Biotechnol.* 2018, 93, 887–896.
- (48) Shiflett, M. B.; Shiflett, A. D.; Yokozeki, A. Separation of tetrafluoroethylene and carbon dioxide using ionic liquids. *Sep. Purif. Technol.* 2011, *79*, 357–364. (49) Shiflett, M. B.; Yokozeki, A. Separation of
- (49) Shiflett, M. B.; Yokozeki, A. Separation of difluoromethane and pentafluoroethane by extractive distillation using ionic liquid. *Chem. Today* 2006, *24*, 28–30.
- (50) Asensio-Delgado, S.; Pardo, F.; Zarca, G.; Urtiaga, A. Absorption separation of fluorinated refrigerant gases with ionic liquids: Equilibrium, mass transport, and process design. *Sep. Purif. Technol.* 2021, *276*, 119363.
- design. Sep. Purif. Technol. 2021, 276, 119363. (51) Lemmon, E. W.; Bell, I. H.; Huber, M. L.; McLinden, M. O. NIST Standard Reference Database 23: Reference Fluid Thermodynamic and Transport Properties-REFPROP, Version 10.0; National Institute of Standards and Technology: Gaithersburg, 2018.
- (52) Barley, M. H.; Morrison, J. D.; O'Donnel, A.; Parker, I. B.:
- Petherbridge, S.; Wheelhouse, R. W. Vapour-liquid equilibrium data for binary mixtures of some new refrigerants. *Fluid Phase Equilib.* 1997, *140*, 183–206.
- (53) Shiflett, M. B.; Yokozeki, A.; Knapp, J. P. Process for the
- Separation of Fluorocarbons Using Ionic Liquids. U.S. Patent 7,964,760 B2, 2011.
- (54) Shiflett, M. B.; Yokozeki, A. Utilizing Ionic Liquids for Hydrofluorocarbon Separation. U.S. Patent 2007/0131535 A1, 2007.
- (55) Beste, Y. A.; Schoenmakers, H. Distillative Method for Separating Narrow Boiling or Azeotropic Mixtures Using Ionic Liquids. U.S. Patent 2007/0080052 A1, 2007.
- (56) Shiflett, M. B.; Yokozeki, A. Solubility and Diffusivity of Hydrofluorocarbons in Room-Temperature Ionic Liquids. *AIChE J.* 2006, *52*, 1205–1219.
- AIChE J. 2006, 52, 1205–1219.

 (57) Morais, A. R. C.; Harders, A. N.; Baca, K. R.; Olsen, G. M.; Befort, B. J.; Dowling, A. W.; Maginn, E. J.; Shiflett, M. B. Phase Equilibria, Diffusivities, and Equation of State Modeling of HFC-32 and HFC-125 in Imidazolium-Based Ionic Liquids for the Separation of R-410A. Ind. Eng. Chem. Res. 2020, 59, 18222–18235.
- (58) Li, L.; Huang, X.; Jiang, Q.; Xia, L.; Wang, J.; Ai, N. New process development and process evaluation for capturing CO2 in flue gas from power plants using ionic liquid [emim][Tf2N]. Chin. J. Chem. Eng. 2020, 28, 721–732.
- (59) Jiqin, Z.; Jian, C.; Chengyue, L.; Weiyang, F. Viscosities and Interfacial Properties of 1-Methyl-3-butylimidazolium Hexafluoro- phosphate and 1-Isobutenyl-3-methylimidazolium Tetrafluoroborate Ionic Liquids. *J. Chem. Eng. Data* 2007, *52*, 812–816.
- (60) Cao, Y.; Mu, T. Comprehensive Investigation on the Thermal Stability of 66 Ionic Liquids by Thermogravimetric Analysis. *Ind. Eng. Chem. Res.* 2014, *53*, 8651–8664.
- (61) Feng, W.-q.; Lu, Y.-h.; Chen, Y.; Lu, Y.-w.; Yang, T. Thermal stability of imidazolium-based ionic liquids investigated by TG and FTIR techniques. *J. Therm. Anal. Calorim.* 2016, *125*, 143–154.
- (62) Chancelier, L.; Boyron, O.; Gutel, T.; Santini, C. Thermal stability of imidazolium-based ionic liquids. *Fr.-Ukr. J. Chem.* 2016, *4*, 51–64.
- (63) Freire, M. G.; Neves, C. M. S. S.; Marrucho, I. M.;

Coutinho, J.

A. P.; Fernandes, A. M. Hydrolysis of Tetrafluoroborate and Hexafluorophosphate Counter Ions in Imidazolium-Based Ionic Liquids. *J. Phys. Chem. A* 2010, *114*, 3744–3749.

- (64) Jia, T.; Bi, S.; Wu, J.; Li, P. Solubilities of difluoromethane (R32) in polyol ester, polyvinylether, and polyalkylene glycol base oils at temperatures from 273 K to 351 K. *Int. J. Refrig.* 2020, *111*, 63–70. (65) Wahlström, Å.; Vamling, L. Solubility of HFCs in
- (65) Wahlström, Å.; Vamling, L. Solubility of HFCs in Pentaerythritol Tetraalkyl Esters. *J. Chem. Eng. Data* 2000, *45*, 97–103.
- (66) Jia, X.; Wang, J.; Hu, Y.; Sun, Y.; Wang, X. Solubilities of R32 in Polyol Ester and Polyvineyl Ether from 278.15 to 348.15 K. *J. Chem. Eng. Data* 2020, 65, 4306–4317.
- (67) Morais, A. R. C.; Simoni, L. D.; Douglas, J. T.; Scurto, A. M.; Shiflett, M. B. Phase equilibrium and diffusivities of hydro-fluorocarbons in a synthetic polyol ester lubricant. *AIChE J.* 2020, *66*, 16241.
- (68) Peng, D.-Y.; Robinson, D. B. A New Two-Constant Equation of State. *Ind. Eng. Chem. Fundam.* 1976, *15*, 59–64.
- (69) Mathias, P. M.; Klotz, H. C.; Prausnitz, J. M. Equation-of-State mixing rules for multicomponent mixtures: the problem of invariance. *Fluid Phase Equilib.* 1991, *67*, 31–44.
- (70) Valderrama, J. O.; Rojas, R. E. Critical Properties of Ionic Liquids. Revisited. *Ind. Eng. Chem. Res.* 2009, 48, 6890–6900.
- (71) Valderrama, J. O.; Robles, P. A. Critical Properties, Normal Boiling Temperatures, and Acentric Factors of Fifty Ionic Liquids. *Ind. Eng. Chem. Res.* 2007, 46, 1338–1344
- (72) Ge, R.; Hardacre, C.; Jacquemin, J.; Nancarrow, P.; Rooney, D. W. Heat Capacities of Ionic Liquids as a Function of Temperature at
- 0.1 MPa. Measurement and Prediction. *J. Chem. Eng. Data* 2008, *53*, 2148–2153.
- (73) Shiflett, M. B.; Yokozeki, A. Vapor-Liquid-Liquid Equilibria of Pentafluoroethane and Ionic Liquid [bmim][PF6] Mixtures Studied with the Volumetric Method. *J. Phys. Chem. B* 2006, 110, 14436–14443.
- (74) Shiflett, M. B.; Yokozeki, A. Vapor-Liquid-Liquid Equilibria of Hydrofluorocarbons + 1-Butyl-3-methylimidazolium Hexafluorophos- phate. *J. Chem.*

- Eng. Data 2006, 51, 1931-1939.
- (75) Shiflett, M. B.; Yokozeki, A. Binary Vapor-Liquid and Vapor- Liquid-Liquid Equilibria of Hydrofluorocarbons (HFC-125 and HFC- 143a) and Hydrofluoroethers (HFE-125 and HFE-143a) with Ionic Liquid [emim][Tf2N]. *J. Chem. Eng. Data* 2008, *53*, 492–497.
- (76) Shiflett, M. B.; Yokozeki, A. Solubility Differences of Halocarbon Isomers in Ionic Liquid [emim][Tf2N]. *J. Chem. Eng. Data* 2007, *52*, 2007–2015.
- (77) Minnick, D. L.; Shiflett, M. B. Solubility and Diffusivity of Chlorodifluoromethane in Imidazolium Ionic Liquids: [emim]-[Tf2N], [bmim][BF4], [bmim][PF6], and [emim][TFES]. *Ind. Eng. Chem. Res.* 2019, *58*, 11072–11081.
- (78) Peng, J.; Edgar, T. F.; Bruce Eldridge, R. Dynamic Rate-Based and Equilibrium Model Approaches for Continuous Tray Distillation Column. *Chem. Eng. Sci.* 2003, *58*, 2671–2680.
- (79) Bravo, J. L.; Fair, J. R. Generalized Correlation for Mass Transfer in Packed Distillation Columns. *Ind. Eng. Chem. Process Des. Dev.* 1982, *21*, 162–170.
- (80) Toor, H. L. Prediction of Efficiencies and Mass Transfer on a Stage with Multicomponent Systems. *AIChE J.* 1964, *10*, 545–548.
- (81) Mu'ller, N. P.; Segura, H. An overall rate-based stage model for cross flow distillation columns. *Chem. Eng. Sci.* 2000, *55*, 2515–2528.
- (82) Lee, Y. S.; Kim, M. G.; Ha, D. M.; Oda, A.; Ito, C.; Aragaki, T.; Mori, H. Analysis of packed distillation columns with a ratebased model. *Korean J. Chem. Eng.* 1997, *14*, 321–324.
- (83) Quijada-Maldonado, E.; Meindersma, G. W.; de Haan, A. B. Ionic liquid effects on mass transfer efficiency in extractive distillation of water-ethanol mixtures. *Comput. Chem. Eng.* 2014, *71*, 210–219.
- (84) Song, D.; Seibert, A. F.; Rochelle, G. T. Mass Transfer Parameters for Packings: Effect of Viscosity. *Ind. Eng. Chem. Res.* 2018, *57*, 718–729.
- (85) Quijada-Maldonado, E.; Aelmans, T. A. M.; Meindersma, G. W.; de Haan, A. B. Pilot plant validation of a rate-based extractive distillation model for water-ethanol separation with the ionic liquid [emim][DCA] as solvent. *Chem. Eng. J.* 2013, *223*, 287–297.

Ind. Ena. Chem. Res. XXXX, XXX.

- (86) Rocha, J. A.; Bravo, J. L.; Fair, J. R. Distillation Columns Containing Structured Packings: A Comprehensive Model for Their Performance. 1. Hydraulic models. *Ind. Eng. Chem. Res.* 1993, *32*, 641–651.
- (87) Rocha, J. A.; Bravo, J. L.; Fair, J. R. Distillation Columns Containing Structured Packings: A Comprehensive Model for Their Performance. 2. Mass-Transfer Model. *Ind. Eng. Chem. Res.* 1996, *35*, 1660–1667.
- (88) Tariq, M.; Serro, A. P.; Mata, J. L.; Saramago, B.; Esperanca J. M. S. S.; Canongia Lopes, J. N.; Rebelo, L. P. N. Hightemperature surface tension and density measurements of 1-alkyl-3-methylimida-zolium bistriflamide ionic liquids. *Fluid Phase Equilib.* 2010, 294, 131–138.
- (89) Paulechka, Y. U.; Blokhin, A. V.; Kabo, G. J.; Strechan, A. A. Thermodynamic properties and polymorphism of 1-alkyl-3-methyl- imidazolium bis(triflamides). *J. Chem. Therm.* 2007, 39. 866–877.
- (90) Kabo, G. J.; Blokhin, A. V.; Paulechka, Y. U.; Kabo, A. G.; Shymanovich, M. P.; Magee, J. W. Thermodynamic Properties of 1- Butyl-3-methylimidazolium Hexafluorophosphate in the Condensed State. *J. Chem. Eng. Data* 2004, 49, 453–461.
- (91) Pereiro, A. B.; Legido, J. L.; Rodríguez, A. Physical properties of ionic liquids based on 1-alkyl-3-methylimidazolium cation and hexafluorophosphate as anion and temperature dependence. *J. Chem. Therm.* 2007, 39, 1168–1175.
- (92) Freire, M. G.; Carvalho, P. J.; Fernandes, A. M.; Marrucho, I. M.; Queimada, A. J.; Coutinho, J. A. P. Surface tensions of imidazolium based ionic liquids: Anion, cation, temperature and water effect. *J. Colloid Interface Sci.* 2007, 314, 621–630.
- (93) Sulzer. www.sulzer.com (accessed Sept 13, 2021).
- (94) Shankland, I. R.; Atwood, T.; Lund, E. A. E.; Pham, H. T. Azeotrope-Like Compositions of Pentafluoroethane and 1,1,1-Trifluoroethane. U.S. Patent 5,211,867 A, 1993.
- (95) Shankland, I. R.; Lund, E. A. E. Azeotrope-Like Compositions of Pentafluoroethane and Difluoromethane. U.S. Patent 4,978,467 A, 1990.